

An RF Circuit Model for Interdigital Capacitors-Based Carbon Nanotube Biosensors

Hee-Jo Lee, *Student Member, IEEE*, Hyun-Seok Lee, Hyang Hee Choi, Kyung-Hwa Yoo,
and Jong-Gwan Yook, *Member, IEEE*

Abstract—We present improved RF circuit modeling of a biosensing element based on a single-walled carbon nanotube combined interdigital capacitors at microwave frequencies. From the resultant circuit, the lumped element values for biomolecular binding are accurately obtained. It is thereby found that the completed RF circuit model shows excellent agreement with measured results. This implies that the electrical properties of a specific biomolecular binding system can be quantitatively analyzed if an optimal RF circuit model is constructed. Finally, we suggest that the suggested methodology can be used to analyze other biomolecular sensing methods.

Index Terms—Biosensor, carbon nanotube (CNT), interdigital capacitors (IDCs), microwave, resonant frequency.

I. INTRODUCTION

IN the past decade, carbon nanotubes (CNTs) have received considerable attention for potential application in nanosized electronic devices owing to their inherent properties of small size, high mechanical strength, high electrical and thermal conductivity, and high surface area [1], [2]. CNTs can be either metallic or semiconducting and their electrical properties can rival or even exceed the best-known semiconductors or metals [3]. Semiconducting CNTs have been mainly used for nanotube field effect transistors (NTFETs) [4], [5] and metallic CNTs have been considered as interconnects for very large-scale integration circuits [6], [7]. CNTs have been particularly well defined with respect to application in NTFET devices, and the effects of small molecules, relative humidity, and conductive liquid media on CNT-based NTFET have been estimated [8]–[10].

Biosensing applications using NTFETs (e.g., an immunoassay for α -fetoprotein [11], sensitive pH sensing [12], and DNA detection [13]) have been extensively investigated. However, there are two major drawbacks in using CNT biosensors based on change of resistance (or conductance): long recovery time (up 10 h) and the contact requirements. Recently, from the viewpoint of RF (or microwave), CNT-based electromagnetic resonator

sensors that exhibit sensitivity to a variety of gases have been demonstrated [14], [15]. The recovery times of these sensors are less than 10 min. In addition, the sensors does not require two-terminals or higher-contacts for measurement. Although the sensors have the aforementioned advantages, they still carry the key disadvantage of low sensitivity. Similarly, CNT sensors based on LC resonators (fabricated by combining an inductor and capacitor device) suffer similar limitations owing to low sensitivity when used for biomolecular detection [16], [17].

In a previous paper [18], we employed a semiconducting single-walled carbon nanotube (SWNT) in conjunction with an interdigital capacitors (IDCs), a type of RF passive element, to produce a high-sensitivity biosensing element for the microwave region. We have demonstrated the feasibility of the proposed biosensor using the resonant frequency change of the S_{11} -parameter. Furthermore, an equivalent RF circuit model has been developed to attain better understanding of the biomolecular sensing mechanism of the device. The previous RF circuit modeling, however, was mainly focused on the resonant frequency behavior of the S_{11} -parameter only, in conjunction with biomolecular binding. As a result, the resulting circuit had limited success in interpreting the biomolecular sensing mechanism as a resonant frequency change. Recently, it has been found that to construct a more accurate RF equivalent circuit model to understand the resonant frequency as a function of biomolecular binding in the biosensor, the modeling procedure should take into account the behaviors of the S_{21} - (or S_{12} -) parameter as well as the RF characteristics of IDCs at high frequencies.

In this paper, we investigate the RF characteristics of IDCs at high frequency and propose an improved RF equivalent circuit for IDCs-based CNT biosensors. From the resulting circuit model, we obtain electrical values of the lumped elements and show that the self-resonant frequency (SRF) can be attributed to differences between the various processes of biomolecular binding onto the CNT.

II. FABRICATIONS AND MEASUREMENTS OF IDCs WITH CNT

A. IDCs and SRF

An IDCs is a kind of passive capacitor element that produces high capacitance and passes high frequency. Long finger conductors of the capacitors provide coupling effect between the input and output ports, as shown in Fig. 1. Since the conductors are mounted on a substrate, their height and dielectric constant affect the capacitors' performance. In addition, the thickness of the conductor and its resistivity also affect the electrical characteristics. Meanwhile, for a capacitor element, its impedance

Manuscript received April 20, 2009; accepted September 20, 2010. Date of publication September 29, 2010; date of current version November 10, 2010. This work was supported by the Ministry of Knowledge and Economy, Korea, under the Information Technology Research Center supported program IITA-2009-C1090-0801-0038. The review of this paper was arranged by Associate Editor L.-E. Wernersson.

H.-J. Lee and J.-G. Yook are with the Department of Electrical and Electronic Engineering, Yonsei University, Seoul 120-749, Korea (e-mail: heejois@yonsei.ac.kr; jgyook@yonsei.ac.kr).

H.-S. Lee and K.-H. Yoo are with the Department of Physics, Yonsei University, Seoul 120-749, Korea (e-mail: s25k@phy.yonsei.ac.kr; khyoo@yonsei.ac.kr).

H. H. Choi is with the Yonsei Nanomedical Core Research Center, Yonsei University, Seoul 120-749, Korea (e-mail: netchoi@yonsei.ac.kr).

Digital Object Identifier 10.1109/TNANO.2009.2033271

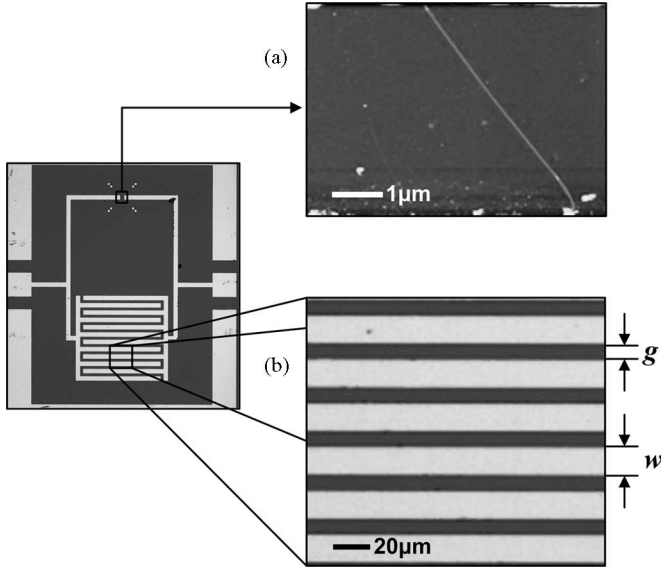


Fig. 1. Photograph of the proposed biosensor device ($940 \times 1180 \mu\text{m}^2$). (a) AFM image of a SWNT in the $5 \mu\text{m}$ upper gap. (b) Multiple finger periodic pattern in the IDCs (the gap between fingers and the width of fingers are $g = 10 \mu\text{m}$ and $w = 20 \mu\text{m}$, respectively).

behaves as would be expected from the specified capacitance at low frequencies. However, the capacitive and parasitic inductive impedance cancel each other out leaving only a resistive component at high frequencies. The critical frequency is the so-called SRF. Above this frequency, inductive reactance becomes dominant, as it becomes much larger than the capacitive reactance and the resistive components.

B. Design and Fabrication of IDCs With CNT

In this study, IDCs have been designed to have self-resonant behavior at 10 GHz. The frequency can be predicted using

$$f_r = \frac{1}{2\pi\sqrt{LC}} \quad (1)$$

where f_r is the resonant frequency, L is the parasitic inductance, and C is the designed capacitance. As a result, the IDCs-based CNT device itself can be regarded as a novel CNT biosensors based on frequency change for biomolecular sensing at the microwave regime.

In this paper, Au pads of $0.1 \mu\text{m}$ thickness were fabricated on heavily doped Si substrates with a 500 nm thick grown SiO_2 layer via photolithography and lift-off techniques. The CNTs bridging the upper gap of the metal pad were fabricated by a patterned catalyst growth technique. First, cocatalyst islands were patterned on a SiO_2/Si substrate, and CNTs were grown by chemical vapor deposition using a mixture of methane and argon as a carbon source at 900°C . Next, the metal pad was found to cover the catalyst islands. Finally, CNTs were grown in parallel with an IDCs, as shown in Fig. 1(a).

Topologically, the gaps between the fingers and the width of the fingers of IDCs are 10 and $20 \mu\text{m}$, respectively. Here, the length of fingers is also specified as $350 \mu\text{m}$ in Fig. 1(b). Meanwhile, the extended upper gap from the IDCs is $5 \mu\text{m}$. The gap is only placed with a semiconducting SWNT.

C. Experimental Results of IDCs-Based CNT Biosensors

For experimental study, we immobilized biomolecules on the CNT surface as follows: first, the CNT device was placed in 6 mM 1-pyrenbutanoic acid succinimidyl ester (Aldrich) in dimethylformamide (DMF) for 1 h under stirring and then washed with clean DMF, where 1-pyrenbutanoic acid succinimidyl ester was used as a linking molecule. The device was then immersed in phosphate buffered solution (PBS, Aldrich) overnight to fix the biotin molecules to the CNT surface. Finally, the freshly biotinlyted device was immersed in a 100 mg/mL streptavidin in PBS solution for 6 h at room temperature. The streptavidin was immobilized onto the CNT surface by strong intermolecular attraction with biotin.

Each sample is measured with an RF probe tip (40A-GSG-200-P, GGB) and a probe station system (PM5HF, Karl Suss) associated with a vector network analyzer (PNA E8364A, Agilent). The power level was maintained at 0 dBm and the IF was set at 2 kHz for the network analyzer, and full two-port calibration was executed with a short-open-load-through calibration method using a calibration substrate (CS-5, GGB).

In this paper, four different configurations are considered and studied: the IDCs alone, a CNT, a biotinlyted CNT, and biotin-streptavidin binding onto a CNT. For the IDCs alone, the frequency is measured as about 10.02 GHz . When a single CNT is placed in the upper gap region of the IDCs, the frequency is changed to 11.02 GHz . This frequency change is due to occurrence of an electrical short, and consequently, the capacitance is very small. Thus, the resonant frequency between the IDCs alone (f_{REF}) and the IDCs with a CNT (f_{CNT}) is dramatically shifted by $\Delta f_{\text{REF-CNT}} = 1 \text{ GHz}$. For the case of the biotinlyted CNT (f_B) and biotin-streptavidin binding onto the CNT (f_S), the resonant frequencies are changed to 10.82 and 10.22 GHz , respectively. When biotin is immobilized on a CNT, the observed shift in the SRF is $\Delta f_{B-\text{CNT}} = 200 \text{ MHz}$, while for the case of streptavidin binding with biotin, the resonant frequency shifts by more than 600 MHz (Δf_{S-B}). This implies that the frequency changes are caused by capacitance, parasitic inductance, and resistance over the CNT due to the two different nanosized biomolecular binding systems, which consist of a captured streptavidin layer over uniformly immobilized biotinlyted onto the CNT surface. The frequency shifts upon biomolecular binding suggests that the proposed biosensing mechanism can be an excellent candidate for specific biomolecular sensing in the microwave region.

III. ANALYSIS OF RF CIRCUIT MODEL FOR IDCs-BASED CNT BIOSENSORS AND S-PARAMETERS

To better understand the electrical properties related to the underlying mechanism of resonant frequency changes upon the biomolecular binding onto the CNT surface, a more consistent and accurate RF circuit model is imperative. If the circuit model is completely constructed for the IDCs-based CNT biosensors, we can quantitatively determine the electrical quantities to elucidate the cause of the frequency shift. To this effect, we considered the schematics for the four different configurations, and the RF equivalent circuits were

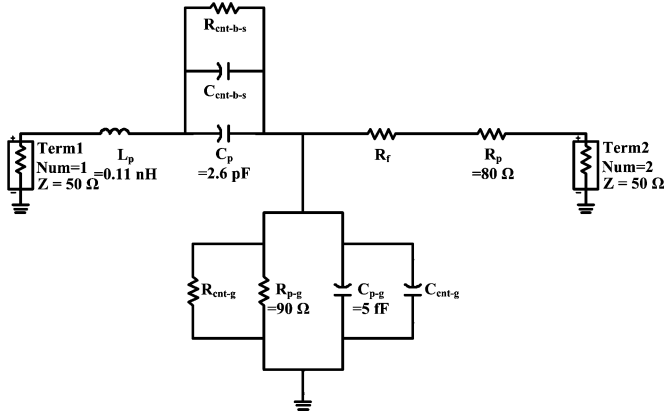


Fig. 2. RF circuit modeling of the IDCs-based CNT biosensor.



Fig. 3. Schematic diagram of two-port network showing network voltage variables.

comprehensively derived as shown in Fig. 2. For constructing the RF circuit model of the IDCs alone without CNTs, the IDCs was simulated via a full electromagnetic simulation based on the moment of method (MOM). With the formulation of the capacitive (4), the capacitance was quantitatively extracted by means of a circuit simulation (ADS, Agilent).

The IDCs-based CNT biosensor can be modeled with a two-port network system as illustrated in Fig. 3 and the biosensor is matched with 50Ω . In this system, the S -parameters are defined in terms of the voltage variables as follows:

$$\begin{aligned} S_{11} &= \left. \frac{V_1^-}{V_1^+} \right|_{V_2^+ = 0} & S_{12} &= \left. \frac{V_1^-}{V_2^+} \right|_{V_1^+ = 0} \\ S_{22} &= \left. \frac{V_2^-}{V_2^+} \right|_{V_1^+ = 0} & S_{21} &= \left. \frac{V_1^-}{V_2^+} \right|_{V_1^+ = 0} \end{aligned} \quad (2)$$

where $V_{n=1,2}^+ = 0$ implies a perfect impedance match (no reflection from terminal impedance) at port n [19]. These definitions may be simply written as

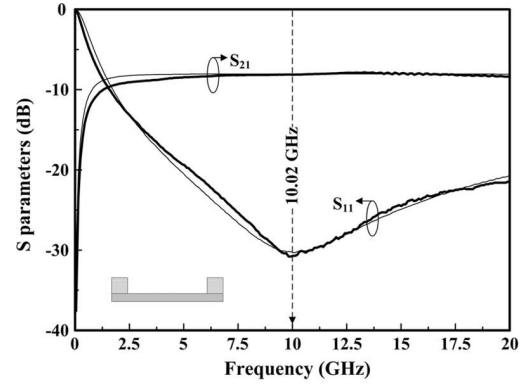
$$\begin{bmatrix} V_1^- \\ V_2^- \end{bmatrix} = \begin{bmatrix} S_{11} & S_{12} \\ S_{21} & S_{22} \end{bmatrix} \begin{bmatrix} V_1^+ \\ V_2^+ \end{bmatrix} \quad (3)$$

and thus, a 2×2 matrix is formed as follows:

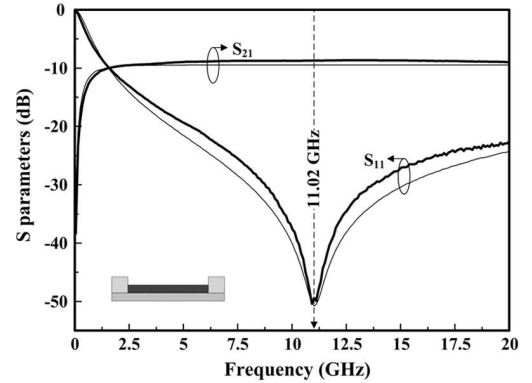
$$[S] = \begin{bmatrix} S_{11} & S_{12} \\ S_{21} & S_{22} \end{bmatrix} \quad (4)$$

where S_{11} (or S_{22}) and S_{21} (or S_{12}) are the ratio of the reflected voltage wave and the transmitted voltage wave to incident voltage wave at port 1 (or port 2), respectively.

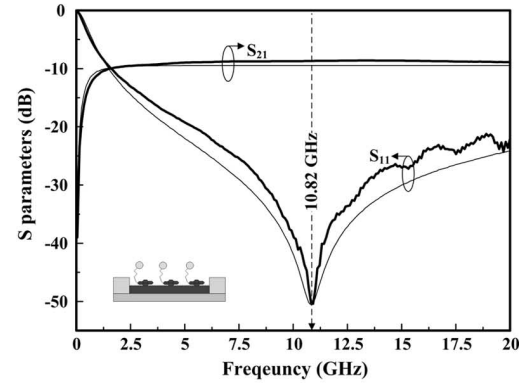
Meanwhile, the explicitly quantitative values of Fig. 2 correspond to the extracted values of the IDCs alone in parallel with



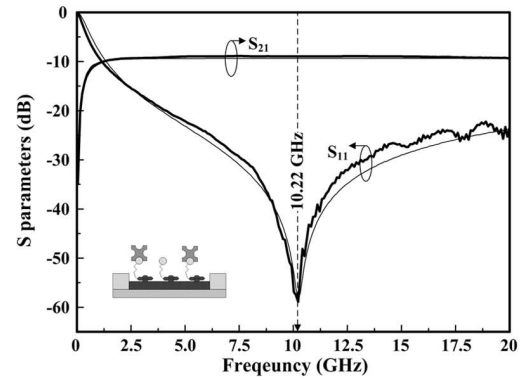
(a)



(b)



(c)



(d)

Fig. 4. Measured (thick solid lines) results and fitting (thin solid lines) results from circuit simulation. (a) IDCs alone with a $5 \mu\text{m}$ upper gap (see inset). (b) CNT in the gap. (c) Biotinlyted CNT. (d) Biotin (circles)–streptavidin (quadrangles with four-binding grooves) binding onto a CNT.

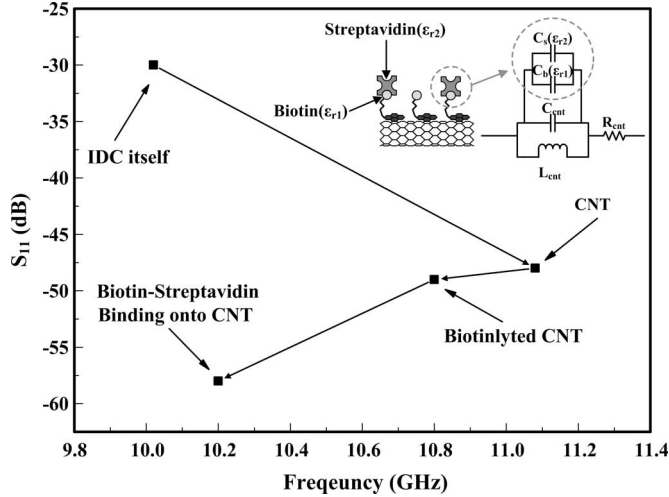


Fig. 5. Frequency change and circuit modeling of biotin (ϵ_{r1})-streptavidin (ϵ_{r2}) binding onto a CNT (inset: upper right).

TABLE I
LUMPED ELEMENT VALUES EXTRACTED BY RF CIRCUIT MODELING

Cases	$R_{\text{cnt-g}}$ (k Ω)	$C_{\text{cnt-g}}$ (fF)	$R_{\text{cnt-b-s}}$ (M Ω)	$C_{\text{cnt-b-s}}$ (pF)	R_f (k Ω)
CNT(bare)	0.5	11	0.462	0.40	19
Biotin	0.5	11	11.80	0.52	19
Streptavidin	0.5	11	0.901	0.87	17.3

a 5 μm upper gap. Here, the pad capacitance (C_p) of the IDCs alone is defined as [20]

$$C_p = \frac{\text{Im}(Y_{11})}{2\pi f} \quad (5)$$

and

$$Y_{11} = \frac{1}{Z_0} \frac{(1 - S_{11})(1 + S_{22}) + S_{12}S_{21}}{(1 + S_{11})(1 + S_{22}) - S_{12}S_{21}} \quad (6)$$

where Y_{11} is the admittance of S_{11} and Z_0 is the characteristic impedance. The pad inductance (L_p) of the IDCs is obtained from (1). In addition, $R_{\text{p-g}}$ and $C_{\text{p-g}}$ are the resistance and capacitance between the pad and ground, respectively. $R_{\text{cnt-b-s}}$ is obtained from direct current resistance measurements, while $C_{\text{cnt-b-s}}$ and R_f are determined by fitting to experimental results for three different configurations, i.e., CNT, biotinlyted CNT, and streptavidin-biotin binding onto CNT. $R_{\text{cnt-g}}$ and $C_{\text{cnt-g}}$ are the resistance and capacitance between the CNT and ground, and they are similarly extracted by fitting to experimental results. With these extracted circuit parameters, the scattering parameters (S_{11} or S_{21}) for configurations are in excellent agreement with the measured data as shown in Fig. 4.

Note that the low transmission characteristics (S_{21}), as illustrated in Fig. 4, are due to various loss mechanisms, such as dielectric, conductor, and leaky wave losses.

The extracted lumped element values of three configurations are summarized in Table I. It is worth noting that there is considerable change in $C_{\text{cnt-b-s}}$. As the streptavidin couples with the biotinlyted CNT, the capacitance increases by more than 67%.

R_f is weighted with a sharpness-related Q -factor characteristic of S_{11} parameters upon biomolecular binding onto the CNT.

Fig. 5 summarizes the frequency characteristics of the four configurations including the bare IDCs, and it is clearly observed that the frequencies shift lower due to high capacitance resulting from the biomolecular permittivity as well as increased intrinsic charge. The net frequency change for the proposed biosensors can be predicted via the following:

$$\Delta f_r = \frac{1}{2\pi\sqrt{L\Delta C}} \quad (7)$$

Interestingly, specific biotin-streptavidin binding onto a CNT can be modeled as parallel capacitors as illustrated in Fig. 4. In the figure, C_b (ϵ_{r1}) and C_s (ϵ_{r2}) represent biotin and streptavidin capacitances, respectively.

IV. CONCLUSION

In conclusion, an improved RF equivalent circuit model of a CNT-resonator-based biosensor at microwave frequencies is presented. In addition, the biomolecular sensing mechanism has been investigated in terms of the SRF of an RF passive component. It was verified that the SRF shift is mainly due to capacitance changes, which in turn are due to different biomolecular binding processes. The proposed biosensor has several advantages: it employs a simple and direct detection mechanism; it is cost-efficient; and it is a label-free technique. Even with these advantages, further studies are necessary for improving the optimal IDCs topology to minimize substrate-related parasitic for lower power loss and to enhance the sensitivity at lower biomolecular concentrations. It is worth mentioning that the novel frequency-based biosensor has potential for wireless remote sensing applications, such as in a biosensing node with an RF transmit system that can transfer information of real-time measurements for biomolecular sensing in a biofluidic state. It can also be applied for detection of other specific biomolecular bindings, such as those involved in antigen-antibody reactions, and DNA hybridization.

REFERENCES

- [1] S. Ijima, "Helical microtubules of graphitic carbon," *Nature*, vol. 354, pp. 56–58, Nov. 1991.
- [2] M. S. Dresselhaus, "Down the straight and narrow," *Nature*, vol. 358, pp. 195–196, Jul. 1992.
- [3] P. L. McEuen, M. S. Fuhrer, and H. K. Park, "Single-walled carbon nanotube electronics," *IEEE Trans. Nanotechnol.*, vol. 1, no. 1, pp. 78–85, Mar. 2002.
- [4] J. A. Misewich, R. Martel, Ph. Avouris, J. C. Tsang, S. Heinze, and J. Tersoff, "Electrically induced optical emission from a carbon nanotube FET," *Science*, vol. 300, no. 5620, pp. 783–786, May 2003.
- [5] A. Star, P. Gabriel, K. Bradley, and G. Grunert, "Electronic detection of specific protein binding using nanotube FET Devices," *Nano Lett.*, no. 3, pp. 459–463, Mar. 2003.
- [6] N. Srivastava and K. Banerjee, "Performance analysis of carbon nanotube interconnects for VLSI applications," in *Proc. IEEE/ACM Int. Conf. Comput.-Aided Des.*, San Jose, 2005, pp. 383–390.
- [7] H. T. Soh, C. F. Quate, A. F. Morpurgo, C. M. Marcus, J. Kong, and H. Dai, "Integrated nanotube circuits: Controlled growth and ohmic contacting of single-walled carbon nanotubes," *Appl. Phys. Lett.*, vol. 75, no. 5, pp. 627–629, Aug. 1999.

- [8] J. Kong, N. R. Franklin, C. W. Zhou, M. G. Chapline, S. Peng, K. Cho, and H. Dai, "Nanotube molecular wires as chemical sensors," *Science*, vol. 287, no. 5453, pp. 622–625, Jan. 2000.
- [9] R. Martel, T. Schmidt, H. R. Shea, T. Hertel, and P. Avouris, "Single- and multi-wall carbon nanotube field-effect transistors," *Appl. Phys. Lett.*, vol. 73, no. 17, pp. 2447–2449, Oct. 1998.
- [10] P. G. Collins, K. Bradley, M. Ishigami, and A. Zettl, "Extreme oxygen sensitivity of electronic properties of carbon nanotubes," *Science*, vol. 287, no. 5459, pp. 1804–1804, Mar. 2000.
- [11] J. N. Wohlstader, J. L. Wilbur, G. B. Sigal, H. A. Biebuyck, M. A. Billadeau, L. Dong, A. B. Fischer, and S. R. Gudiband, "Carbon nanotube-based biosensor," *Adv. Mater.*, vol. 15, no. 14, pp. 1184–1187, Jul. 2003.
- [12] K. Besteman, J. O. Lee, F. G. M. Wiertz, H. A. Heering, and C. Dekker, "Enzyme-coated carbon Nanotubes as single-molecule biosensors," *Nano Lett.*, vol. 3, no. 6, pp. 727–730, May 2003.
- [13] J. Clendenin, J. W. Kim, and S. Tung, "An aligned carbon nanotube biosensor for DNA detection," in *Proc. 3rd IEEE Int. Conf. Nano/Micro Eng. Mol. Syst.*, Bangkok, 2007, pp. 1028–1033.
- [14] S. Chopra, A. Pham, J. Gaillard, A. Parker, and A. M. Rao, "Carbon-nanotube-based resonant-circuit sensor for ammonia," *Appl. Phys. Lett.*, vol. 80, no. 24, pp. 4632–4634, Jun. 2002.
- [15] S. Chopra, A. Pham, J. Gaillard, and A. M. Rao, "Development of RF carbon nanotube resonant circuit sensors for gasremote sensing applications," in *Proc. IEEE MTT-S Microw. Symp.*, Hawaii, 2007, pp. 639–642.
- [16] Y. I. Kim, Y. K. Park, and H. K. Baik, "Development of LC resonator for label-free biomolecule detection," *Sens. Actuator A, Phys.*, vol. 143, no. 2, pp. 279–285, May 2008.
- [17] H. J. Lee and J. G. Yook, "Biosensing using split-ring resonators at microwave regime," *Appl. Phys. Lett.*, vol. 143, no. 2, pp. 279–285, May 2008.
- [18] H. S. Lee, H. J. Lee, H. H. Choi, J. G. Yook, and K. H. Yoo, "Carbon-nanotube-resonator-based biosensors," *Small*, vol. 4, no. 10, pp. 1723–1727, Oct. 2008.
- [19] J. S. Hong and M. J. Lancaster, *Microstrip Filters for RF/Microwave Applications*. New York: Wiley-Interscience, 2001.
- [20] Y. H. Lee, S. N. Lee, J. G. Yook, J. H. Kim, and K. J. Chun, "Accurate characterization of MEM inductors on lossy silicon," *Microw. Opt. Technol. Lett.*, vol. 43, no. 4, pp. 355–358, Nov. 2004.



Hee-Jo Lee (S'06) received the B.S. degree in physics education from Daegu University, Gyeongsan, Korea, in 1998, and the M.S. degree in physics and applied physics from Yonsei University, Seoul, Korea, in 2004. Since 2004, he is working toward the Ph.D. degree with the Department of Electrical and Electronic Engineering, Yonsei University.

His current research interests include the areas of electromagnetic wave theory, solid-state physics, surface plasmonics, metamaterials, photonic crystals, nuclear magnetic resonance, physics of magnetic resonance imaging, nanoelectromagnetics, nanomaterials for biosensors, and nanobiosensors based on carbon nanotube and double split-ring resonator as well as electrical properties and RF circuit modeling of carbon nanotube and graphene at microwave to optical region.

Hyun-Seok Lee received the B.S. degree in physics from Gyonggi University, Suwon, Korea, in 2001, and the M.S. degree in physics and applied physics from Yonsei University, Seoul, Korea, in 2003. Since 2003, he is working toward the Ph.D. degree with the Department of Physics, Yonsei University.

His current research interests include the area of biosensors based on carbon nanotube at microwave system.

Hyang Hee Choi received the Ph.D. degree in chemical engineering from Chosun University, Gwangju, Korea, in 1998.

She was a Postdoctoral Fellow with the University of Massachusetts, Boston, and also with Inha University, Incheon, Korea, during 2000. She has been a Research Professor with the Yonsei Nanomedical Core Research Center, Yonsei University, Seoul, Korea, since 2005. Her current research interests include the area of synthesis and applications of carbon nanotube.

Kyung-Hwa Yoo received the B.S. degree in physics from Yonsei University, Seoul, Korea, in 1982, and the M.S. and Ph.D. degrees in physics from University of Illinois, Urban-Champaign, in 1984 and 1986, respectively.

In 1997, she joined as a Principle Researcher with Korea Research Institute of Standard and Science, Daejeon. Since 2001, she is a Professor with the Department of Physics, Yonsei University, and since 2005, she is the Chairman of Nanomedical National Core Research Center, Yonsei University. Her current research interests include the areas of condensed matter experiment, biophysics, nanobiosensors using electrical properties measurement, carbon nanotube device, single-electron device, molecular device, origin/inorganic hybrid device, and solar cell.



Jong-Gwan Yook (S'89–M'97) was born in Seoul, Korea. He received the B.S. and M.S. degrees in electronics engineering from Yonsei University, Seoul, Korea, in 1987 and 1989, respectively, and the Ph.D. degree from the University of Michigan, Ann Arbor, in 1996.

He is currently a Professor with the Department of Electrical and Electronic Engineering, Yonsei University. His research interests include the areas of theoretical/numerical electromagnetic modeling and characterization of microwave/millimeter-wave circuits and components, design of radio frequency integrated circuits and monolithic microwave integrated-circuit, and analysis and optimization of high-frequency high-speed interconnects, including RF microelectromechanical systems, based on frequency as well as time-domain full-wave methods. His research team has also been engaged in the development of biosensors, such as carbon nanotube radio frequency biosensor for nanometer size antigen-antibody detection as well as remote wireless vital signal monitoring sensors.